Development 102, 193–210 (1988)
Printed in Great Britain © The Company of Biologists Limited 1988

Developmental patterning of carbohydrate antigens during early embryogenesis of the chick: expression of antigens of the poly-*N*-acetyllactosamine series

SUSAN J. THORPE[1], RUTH BELLAIRS[2] and TEN FEIZI[1]

[1]*Applied Immunochemistry Research Group, Clinical Research Centre, Watford Road, Harrow HA1 3UJ, UK*
[2]*Department of Anatomy and Embryology, University College London, Gower Street, London WC1E 6BT, UK*

Summary

This report describes a striking temporal and spatial patterning of specific carbohydrate sequences in the developing chick embryo. By using oligosaccharide sequence-specific monoclonal antibodies as immunohistochemical reagents in conjunction with neuraminidase, it was possible to visualize the occurrence, as well as the changes in distribution, of oligosaccharides of the poly-*N*-acetyllactosamine series. These were (a) long-chain unbranched sequences reactive with anti-i Den, (b) long-chain branched sequences reactive with anti-I Step and (c) short-chain branched sequences reactive with anti-I Ma and (d) their sialylated forms. The salient observations with serial sections of embryos from the unincubated to the 17th stage were as follows.

(1) A pronounced anteroposterior patterning appeared during neuroectodermal development, such that the long-chain unbranched and long-chain branched sequences, which were abundant on the ectoderm of the earlier stages, were replaced by short-chain branched sialo-oligosaccharides in the developing brain and anterior neural tube.

(2) A striking anteroposterior and mediolateral patterning developed in the subectodermal extracellular spaces. The long-chain linear and short-chain non-sialylated sequences demarcated regions favourable for migration of the lateral plate mesoderm.

(3) A distinction was made between the dorsal and ventral routes of the trunk neural crest in that the extracellular matrix of the dorsal route only was associated with long-chain linear and short-chain sialylated branched sequences.

(4) A circumscribed perinotochordal distribution of the short-chain sialylated branched sequences was observed in the region of the future centra of the vertebrae.

(5) An abundance of long-chain linear and long-chain sialylated branched structures was detected in primordial germ cells which permitted their identification during migration.

These observations suggest that oligosaccharides of the poly-*N*-acetyllactosamine series may have roles as short-range, region-specific information factors during morphogenetic events that take place in the developing embryo, and they open the way to the search for recognition proteins (e.g. endogenous lectins) specific for each of these oligosaccharide structures.

Key words: carbohydrate antigens, patterning, chick embryo, cell migration, ectoderm, extracellular matrix, Ii antigens, neural crest, poly-*N*-acetyllactosamine, primordial germ cells.

Introduction

One of the most important problems in developmental biology is to understand the molecular basis of cell interactions that occur during cell differentiation, morphogenesis and tissue organization. Carbohydrate structures seem ideal candidates as mediators of these cell interactions because of their diversity and their cell- and stage-specific patterns of expression during embryogenesis and differentiation

(Feizi, 1981*a*, 1985). Saccharides of the poly-*N*-acetyllactosamine series (based on repeating disaccharide units, Galβ1–4GlcNAc) are widely distributed in diverse cell types (Childs *et al.* 1979, 1980). During embryonic development and cell differentiation in mouse and man, they show pronounced changes in their branching patterns (Feizi, 1981*a*,*b*; Hakomori, 1981; Feizi *et al.* 1982) and in their peripheral substitutions with fucose (Gooi *et al.* 1981; Fukushi *et al.* 1984), sialic acid and galactose (Pennington *et al.* 1985).

Knowledge of the *in situ* distribution of specific carbohydrate structures should not only give us important clues as to their functions, which may then be tested experimentally, but also contribute to our general understanding of cellular interactions. Using a panel of well-characterized monoclonal antibodies, we have now extended studies of the expression of carbohydrate antigens to chick embryos. We have selected the chick embryo for three reasons.

(1) If these carbohydrate antigens do indeed play a fundamental role in cell interactions, they are unlikely to be restricted to mammals but may be expected to be present also in other classes of vertebrates. Birds have the advantage of a relatively close relationship to mammals from both the evolutionary and morphogenetic points of view.

(2) Knowledge of cell and tissue interaction in early development of the chick embryo greatly exceeds that of any mammalian embryo. The possibility of correlating our findings with developmental processes is thus enhanced.

(3) It is important to be able to test our interpretations by studying the distribution of the carbohydrate antigens after experimental interference. The chick is particularly accessible for experimental manipulations, including microsurgery.

We report here observations based on reactivities of chick embryos at stages 1–17 with antibodies directed at specific domains on linear and branched poly-*N*-acetyllactosamine sequences. These include distinct temporal and spatial changes in immunoreactivities which suggest a link between specific glycosylation patterning and morphogenetic events.

Materials and methods

Chick embryos

Hens' eggs were either unincubated or were incubated for periods of up to 72 h, so that the embryos were at stages 1–17 (Table 1), and were dissected from the yolk and membranes in Pannett and Compton's saline (Pannett & Compton, 1924). Specimens were fixed in buffered formol saline (Drury & Wallington, 1967), dehydrated in graded ethanol concentrations, embedded in paraffin wax and serially sectioned at 4 μm. In some embryos (transverse sections), all sections were stained exclusively with one antibody or corresponding control reagents, while in other embryos (transverse and longitudinal section) adjacent sections were stained with each of the antibodies and control reagents.

Monoclonal antibodies

The carbohydrate structures recognized by the monoclonal antibodies used in this study are shown in Table 2. These carbohydrate antigens occur both on glycoproteins and glycolipids (Feizi, 1981*b*; Uemura *et al.* 1983; Gooi *et al.* 1983). Anti-i Den recognizes the unbranched poly-*N*-acetyllactosamine sequence (structure 1) consisting of at least three disaccharide units (Niemann *et al.* 1978; Gooi *et al.* 1984); anti-I Step recognizes the domains on long, branched poly-*N*-acetyllactosamine sequences indicated on structures 2 and 3 (Feizi *et al.* 1979; Uemura *et al.* 1983); anti-I Ma and M18 (the latter was a gift of Dr P. A. W. Edwards) recognize the short, branch-point sequences Galβ1–4GlcNAcβ1–6– (Feizi *et al.* 1971; Gooi *et al.* 1983) which occur as side chains in structures 2–4, or in the core regions (oligosaccharide–peptide junction) of *O*-glycosidically linked oligosaccharides. For immunofluorescence, the antibodies were used as plasma at dilutions of 1:100 (anti-I Ma) and 1:700 (anti-i Den and anti-I Step) or as ascitic fluid at 1:100 dilution (M18 antibody). As negative controls, normal human serum or mouse ascitic fluid containing an irrelevant monoclonal antibody (anti-dust mite) were used.

Immunofluorescence microscopy

Formalin-fixed paraffin-embedded sections (4 μm) were dewaxed in xylene, cleared through decreasing concentrations of ethanol in water and washed in 0·01 M-phosphate-buffered saline (PBS), pH 7·8. For neuraminidase treatment, the dewaxed and cleared sections were incubated overnight at 37°C with neuraminidase from *Vibrio cholerae* (0·2 i.u. ml^{-1} in complete PBS (Dulbecco A+B),

Table 1. *Embryonic material used*

Stage*	Characteristic embryonic features	Number of embryos		
		TS	LS	Total
1–2	Pre- and early primitive streak	11	–	11
3–6	Full primitive streak to early head process	21	1	22
7–10	1–10 pairs somites	13	1	14
11–14	13–23 pairs somites	11	1	12
17	30 pairs somites	9	1	10

* Staging according to Hamburger & Hamilton (1951).

Table 2. *Carbohydrate structures recognized by the monoclonal antibodies used in this study*

Antibodies	Carbohydrate structures recognized	Designation
Anti-i Den	Galβ1–4GlcNAcβ1–3Galβ1–4GlcNAcβ1–3Galβ1–4Glc/GlcNAcβ1–	1
Anti-I Step* & Anti-I Ma	Galβ1–4GlcNAcβ1 → 6 Galβ1–4GlcNAcβ1– ; Galβ1–4GlcNAcβ1 → 3	2
	Galβ1–4GlcNAcβ1 → 6 Galβ1–4GlcNAcβ1– ; Galβ1–4GlcNAcβ1 → 3 Galβ1–4GlcNAcβ1– ; Galβ1–4GlcNAcβ1 → 3	3
Anti-I Ma† & M18	Galβ1–4GlcNAcβ1 → 6 Galβ1– ; 3 ; Galβ1–3/4GlcNAcβ1	4
	Galβ1–4GlcNAcβ1 → 6 GalNAc–O–peptide ; GlcNAcβ1 → 3	5

*Domains on branched poly-*N*-acetyllactosamine structures recognized by anti-I Step are indicated by continuous underlining.

†The short branch-point structures (dotted underlining) recognized by anti-I Ma and M18 occur both on the poly-*N*-acetyllactosamine structures 2 and 3 and on short-branched oligosaccharides in the presence of Galβ1–3/4GlcNAcβ1–3 or GlcNAcβ1–3 linked to the internal galactose of *N*-acetylgalactosamine residues.

Behringwerke, West Germany) and washed with PBS. Indirect immunofluorescence staining, using the human or mouse monoclonal antibodies, followed by fluorescein-conjugated rabbit anti-human IgM (Dako Immunoglobulins, Mercia Brocades Ltd, Weybridge, Surrey) or fluorescein-conjugated rabbit anti-mouse Ig (Nordic Immunological Laboratories, Maidenhead, Berks), respectively, was performed as described previously (Thorpe & Feizi, 1983). The sections were then fixed in PBS containing 4% (w/v) formaldehyde for 15 min at 4°C and mounted in buffered glycerol (PBS:glycerol, 1:9 (v/v) containing 0·22 M-1,4-diazabicyclo [2.2.2] octane (Sigma Chemical Co. Poole, Dorset), pH 8·6 (Johnson *et al.* 1981). Sections were viewed using a Zeiss epifluorescence microscope. Appearance of new areas of immunofluorescence or an increase in intensity of immunofluorescence after neuraminidase treatment of the sections was taken as evidence for the presence of sialylated backbone structures. Where immunofluorescence of the untreated cells was already intense, an increase of immunoreactivity might not have been detectable. Fluorescence and phase-contrast photomicrographs were taken using Ilford HP5 and Panatomic X films, respectively.

Results

*Linear poly-*N*-acetyllactosamine structures recognized by anti-i Den*

Without neuraminidase treatment

At stages 1–4, the i-antigen was detected intracellularly in the entire embryo, as well as at the apical side of the ectoderm, as shown for stage 1 in Fig. 1A. Thereafter, intracellular staining was greatly reduced, except in certain restricted regions (see below) and, as the neural plate formed, there was a progressive loss of immunoreactivity at the apical side of the ectoderm in the midline. By stage 6, the antigen was absent anteriorly over the neural plate (Fig. 2A) but persisted posteriorly over the primitive streak (Fig. 2D). This anteroposterior pattern was maintained in the neural tube as it closed during stages 7–14, with a lack of immunoreactivity except at the apical surface at the caudal end (Fig. 3J). This anteroposterior pattern persisted in the neural tube of the embryos at stage 17 (not shown).

In contrast to the neural tube, the non-neural ectoderm continued to express the antigen on the apical side throughout stages 6–17 (Figs 2A,D, 5). The immunofluorescence tended to be weaker anteriorly (Fig. 4A) than posteriorly (Fig. 3H–K) and was especially intense in the regions destined to become amnion (Fig. 3A–E). In the lateral body folds, strong intracellular immunofluorescence was observed in the ectoderm (Fig. 5A–C). A similar intracellular immunofluorescence was observed in the region of fusion of the amniotic folds (Fig. 3D,E). Some immunofluorescence was visible at the apical side of the chorion shortly after its separation from the amnion (Fig. 3D) but, by stage 17, this had largely disappeared from the chorion whilst remaining in the amnion.

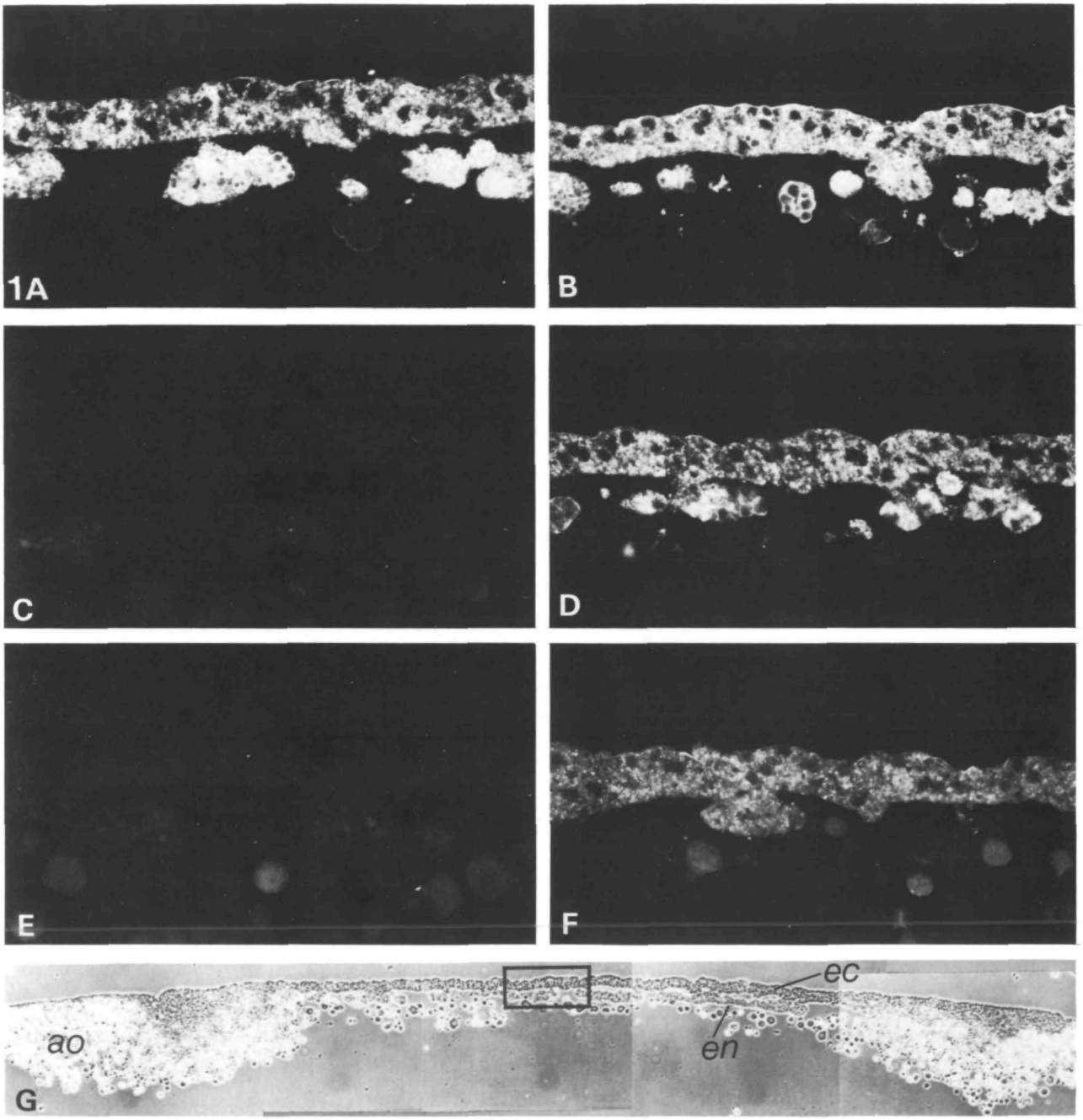

Fig. 1. Fluorescence micrographs of untreated (A,C,E) and neuraminidase-treated (B,D,F) transverse sections of an embryo of stage 1, showing reactivities with anti-i Den (A,B), anti-I Step (C,D) and anti-I Ma (E,F). Reactivity with anti-i Den is enhanced after neuraminidase treatment, whilst reactivities with anti-I Step and anti-I Ma are revealed only after neuraminidase treatment. The region from which panels A–F have been selected is indicated in the boxed area of the phase-contrast micrograph (G). Abbreviations: *ao*, area opaca; *ec*, ectoderm; *en*, endoderm; (A–F) ×276; (G) ×45.

The endoderm at the mid and posterior part of the embryo showed apical surface immunoreactivity from about stage 6 (shown for stage 14 in Fig. 3I–L) but not in the anterior region (Fig. 4A). The intracellular yolk inclusions in the developing area opaca were antigen positive at all stages examined (e.g. Fig. 2A). The extracellular yolk (not shown) was not immunoreactive.

At stages 14–17, restricted areas of immunoreactivity were visible in the following extracellular spaces:

(a) in the regions of the trunk neural crest on the dorsal side of the neural tube (Fig. 3D–F);

(b) in the posterior trunk region beneath the ectoderm, and overlying the somites (Fig. 3H,I) and the proximal part of the lateral plate (not shown);

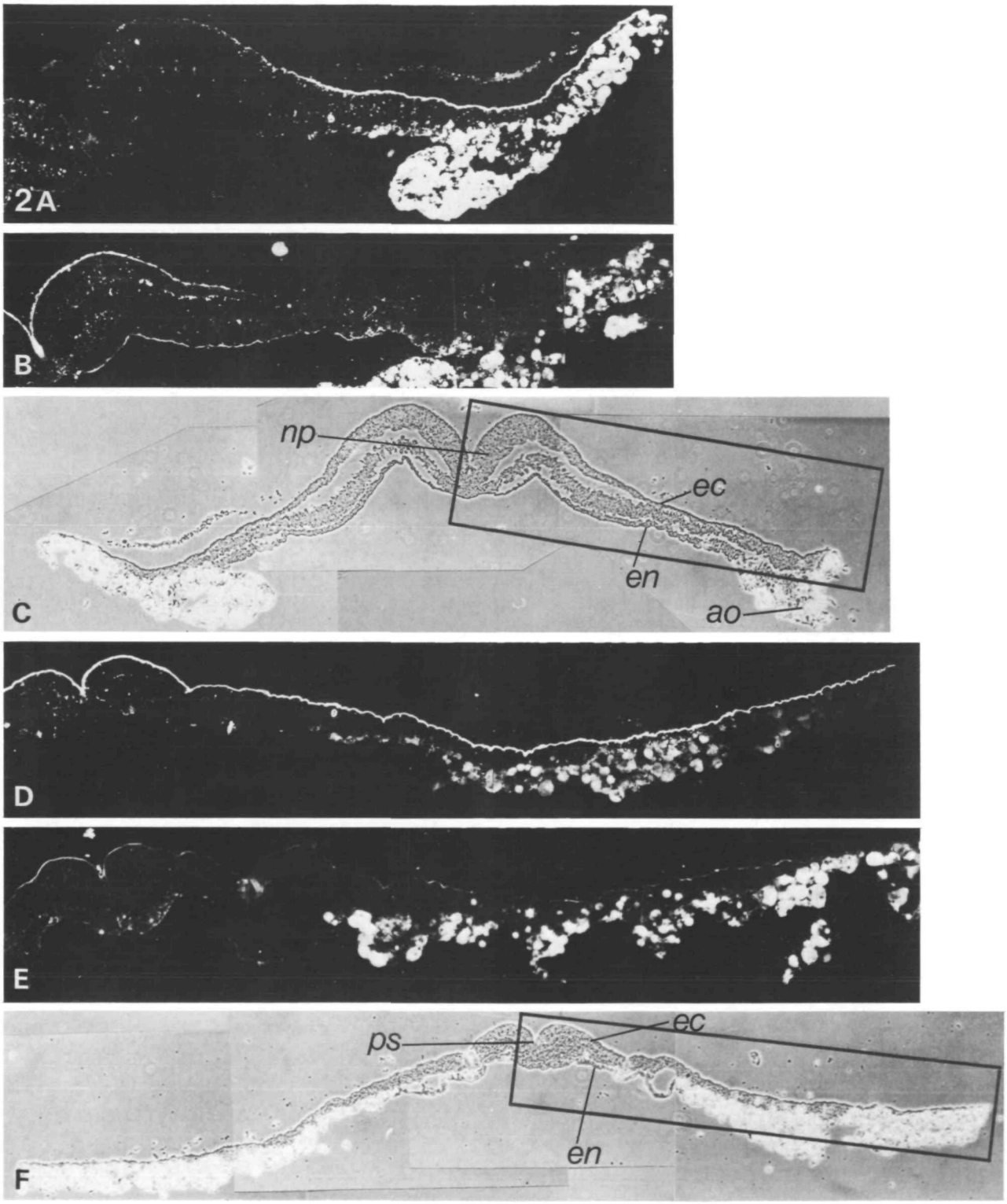

Fig. 2. Photomicrographs of transverse sections across anterior (A–C) and posterior (D–F) regions of a stage-6 embryo showing the reactivities of untreated sections with anti-i Den (A,D) and with neuraminidase-treated sections stained with anti-I Ma (B,E). The region from which panels A and B were taken is indicated in the boxed area of the phase-contrast micrograph C, and that for D and E is indicated in F. There is a reciprocal pattern in the staining of the apical side of the ectoderm in the region of the neural plate: at the anterior end there is negligible staining with anti-i Den and strong staining with anti-I Ma, whilst at the posterior end there is strong staining with anti-i Den and only weak staining with anti-I Ma. *np*, neural plate; *ps*, primitive streak; other abbreviations as in Fig. 1. (A,B,D,E) ×127; (C,F) ×68.

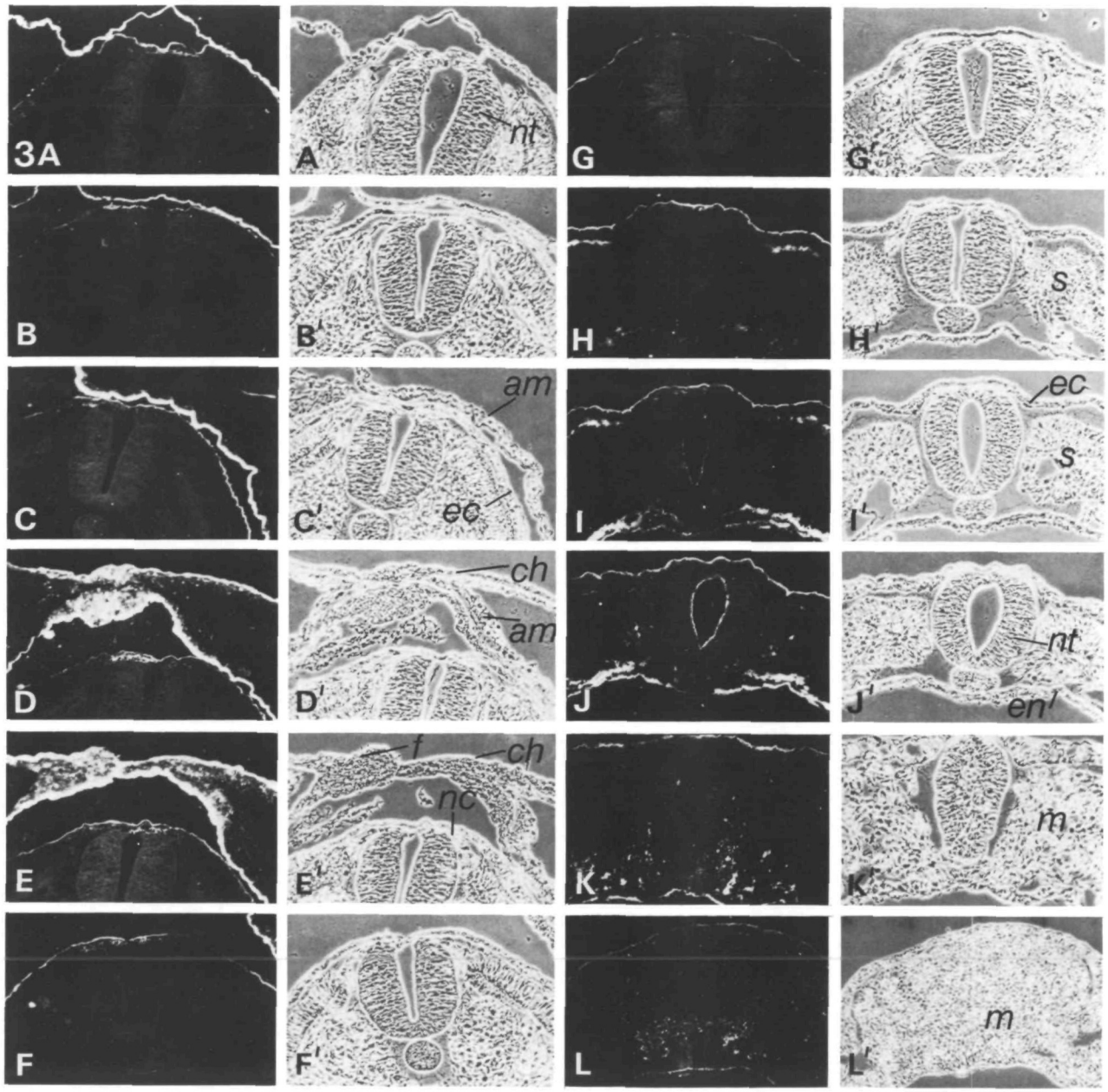

Fig. 3. Fluorescence (A–L) and corresponding phase-contrast (A′–L′) micrographs of transverse sections (selected from serial sections) of a stage-14 embryo stained with anti-i Den and showing (1) The apical side of the neural tube staining at the posterior end (I,J) but not at the anterior end (A–H). (See also Fig. 4A for the cranial end of the same embryo showing a lack of immunofluorescence in the forebrain.) (2) The apical side of the embryonic non-neural ectoderm staining at all levels (e.g. C). (3) The apical sides of amnion and chorion staining strongly, with strong intracellular immunofluorescence in the region of fusion of the amniotic folds (D,E). (4) Extracellular material staining in the region of the neural crest (D–F), laterally between the somites and the overlying ectoderm (H,I), and between mesoderm cells of the tail bud region (K,L). (5) Endoderm staining in the developing hind gut (I–L). Elsewhere this specimen shows areas of tissue autofluorescence. *am*, amnion; *ch*, chorion; *f*, fusion of amniotic folds; *m*, mesoderm; *nc*, neural crest; *nt*, neural tube; *s*, somite. Other abbreviations are as before. Magnification: AA′–KK′, ×122; LL′, ×81.

(c) between the sclerotome cells (Fig. 5D);

(d) around the notochord, with a patchy distribution (Fig. 5D);

(e) around the aortae (Fig. 5D);

(f) between the splanchnic mesoderm and the endoderm (Fig. 5D);

(g) between the mesoderm cells of the tail bud region (Fig. 5E), and beneath the ectoderm at the sides of the tail bud (Fig. 5E).

Certain large cells considered to be primordial germ cells showed strong immunofluorescence. These cells were located mainly in the region of the germinal

crescent (which lies at the anterior border of the area pellucida) from stage 4 to about stage 9 (Fig. 6A). Similar cells were seen in the blood vessels at stages 12–14 (the red blood cells did not show immunoreactivity) (Fig. 6B). From stage 14 to 17, these cells were visible in the splanchnic mesoderm in the midtrunk region (Fig. 6C).

After neuraminidase treatment

Treatment with neuraminidase prior to immunofluorescence staining enhanced the reactivity of the youngest embryos (Fig. 1B) and revealed immunoreactivity at the apical side of the ectoderm and in the cytoplasm of stage-5 embryos in regions previously found to be antigen negative (not shown). No striking differences in immunofluorescence were observed in sections through later embryos (not shown).

*Branched poly-*N*-acetyllactosamine structures recognized by anti-I Step*

Without neuraminidase treatment

Immunofluorescence was detected at the apical side of the embryonic ectoderm only from about stage 12 and this was restricted to the region of the lateral body folds, the apical side of the amnion and the amniotic folds (not shown).

After neuraminidase treatment

The distribution of immunoreactivity (referred to as sialosyl-I Step) at stages 1–4 (Fig. 1D), and the progressive loss at the apical side of the ectoderm along the anteroposterior axis of the body (not shown), resembled the pattern found with anti-i Den up to stage 7. Thereafter, the entire neural tube was lacking in immunoreactivity although the non-neural embryonic ectoderm continued to react patchily, but

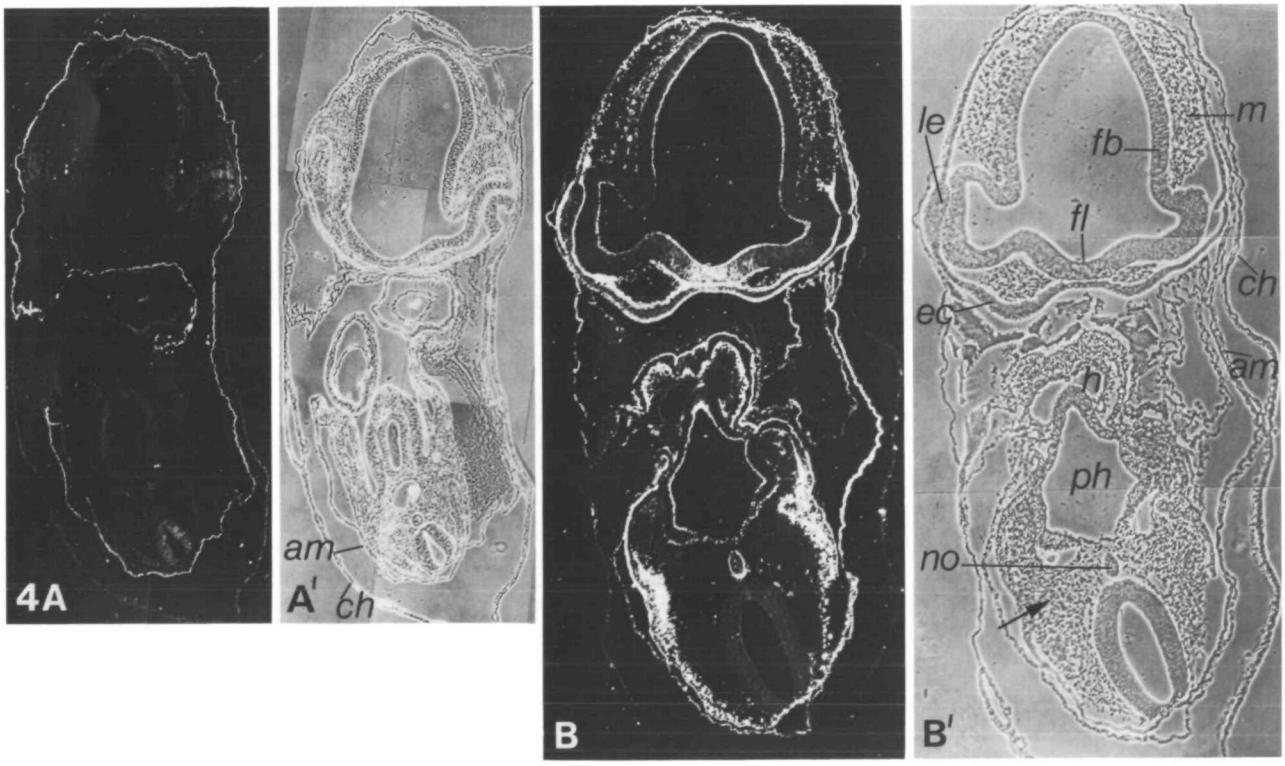

Fig. 4. Fluorescence (A,B) and corresponding phase-contrast (A′,B′) photomicrographs of sections through the anterior ends of two stage-14 embryos stained with anti-i Den (untreated section, A), and anti-I Ma (neuraminidase-treated section, B). Specimen AA′ is the cranial end of the embryo illustrated in Fig. 2. Panel A shows that immunoreactivity with anti-i Den is predominantly at the apical side of the amnion. The immunofluorescence of the non-neural ectoderm is weak; elsewhere there is some tissue autofluorescence. By contrast, immunoreactivity with anti-I Ma was observed at (1) The luminal and basal aspects of the forebrain, and in a localized intra- and pericellular distribution at the floor of the forebrain. (2) The basal and apical sides of the lens placodes. (3) The apical side of the non-neural embryonic and amniotic ectoderm. (4) The apical side of the pharyngeal endoderm. (5) Some extracellular material in the region of head mesoderm at the level of the forebrain, between the heart and anterior body wall, around the notochord, and especially in the region of the future pharyngeal arches (arrowed). *ch*, chorion; *fb*, forebrain; *fl*, floor of forebrain; *h*, heart; *le*, lens placode; *no*, notochord; *ph*, pharynx. Other abbreviations as before. (AA′) ×51; (BB′) ×82.

the extraembryonic ectoderm showed intense immunofluorescence at the apical side of the amnion and the amniotic folds (not shown).

Some major differences in the distribution of sialosyl-I Step from that of i-antigen were as follows. (1) Negligible immunofluorescence was observed in the embryonic endoderm. (2) No immunofluorescence was seen in the extracellular spaces. (3) Immunofluorescence in the primordial germ cells was apparent only until about stage 8; cells corresponding

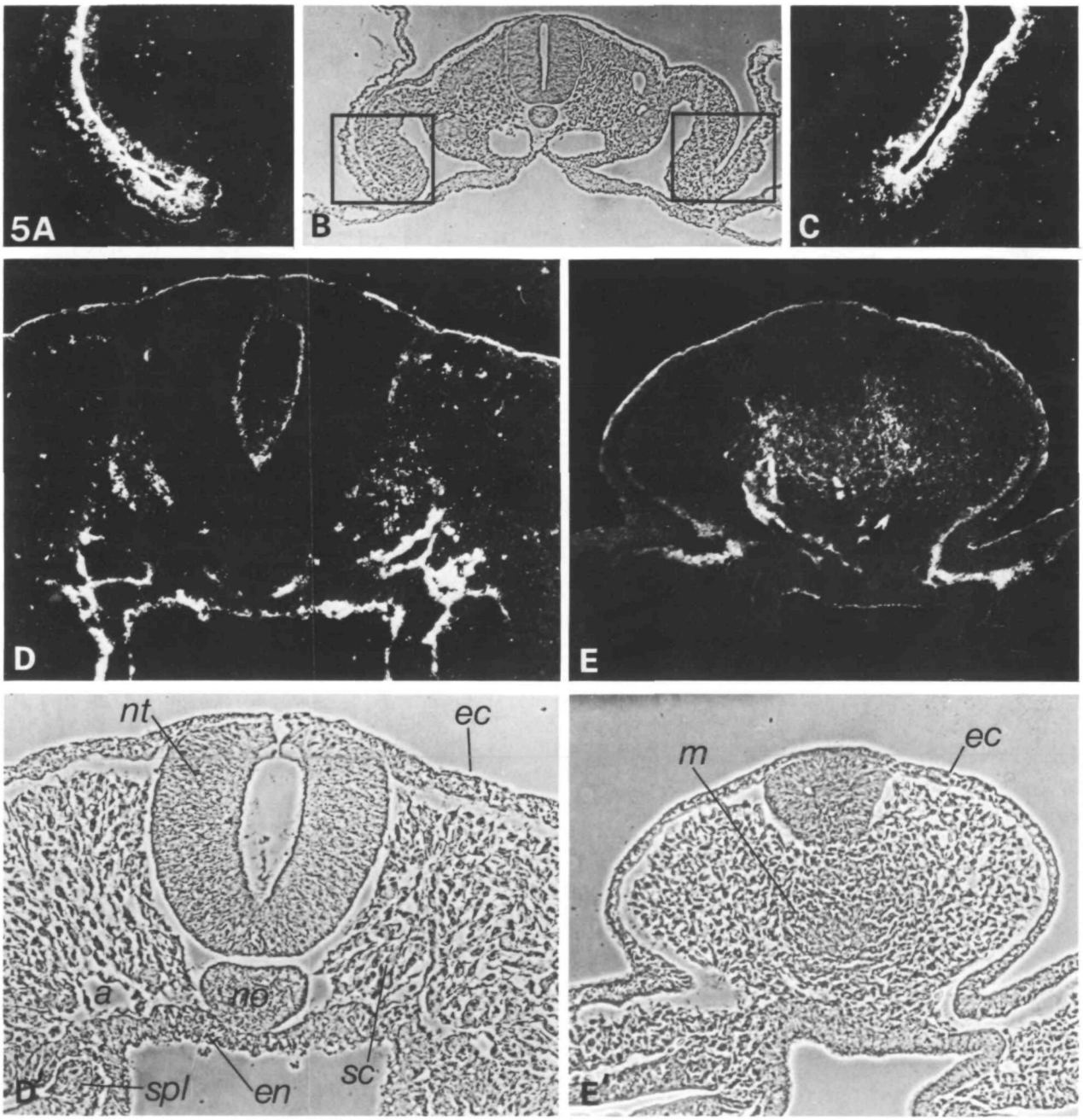

Fig. 5. Fluorescence (A,C–E) and corresponding phase contrast (B′,D′,E′) photomicrographs of transverse sections (selected from serial sections) through a stage-17 embryo stained with anti-i Den. Panels A and C illustrate intracellular and surface staining of ectoderm in the lateral body folds in the midtrunk region. Boxes in panel B correspond to panels A and C. Further caudally, there is staining of the apical side of the neural tube (D) and non-neural ectoderm (D,E); between the sclerotome cells (D); patchily around the notochord (D); around the aortae (D); between the splanchnic mesoderm and endoderm (D); at the apical side of the endoderm in the hind gut (D,E); and between the mesoderm cells in the tail bud (E). *a*, aorta; *scl*, sclerotome; *spl*, splanchnic mesoderm. Other abbreviations as before. (A,C) ×204; (B) ×39, (D,D′) ×198; (EE′) ×124.

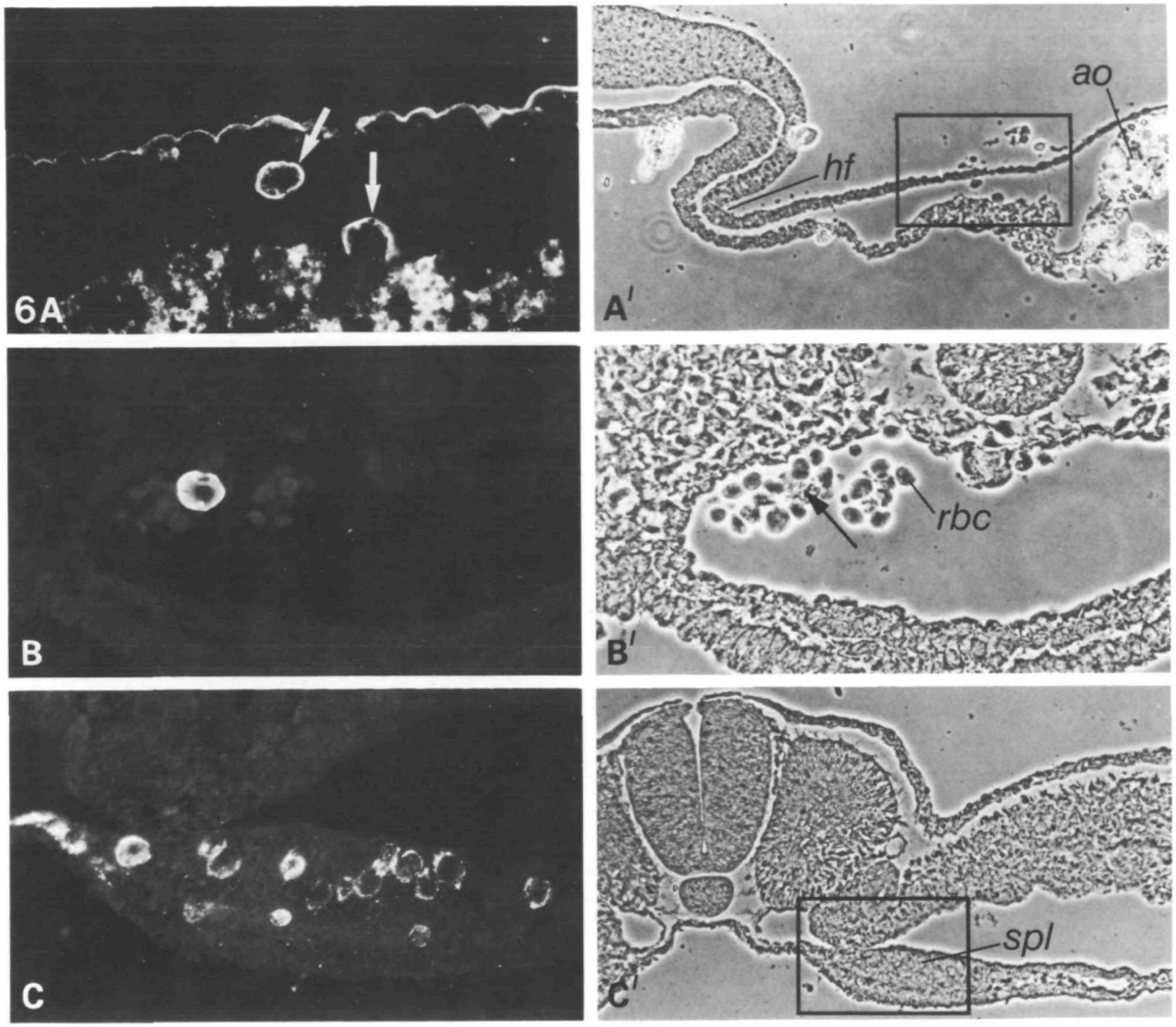

Fig. 6. Fluorescence (A,B,C) and corresponding phase-contrast (A′,B′,C′) photomicrographs showing primordial germ cells stained with anti-i Den. Panel A shows strong pericellular fluorescence of two primordial germ cells (arrowed) in a longitudinal section through the germinal crescent of a stage-6 embryo. This area corresponds to the box in panel A′. Panel B shows fluorescence of a primordial germ cell (arrowed in panel B′) in the aorta of a transverse section of a stage-14 embryo; red blood cells are unreactive. Panel C shows fluorescence of a group of primordial germ cells in the splanchnic mesoderm of the midtrunk region of a transverse section of a stage-17 embryo. This area corresponds to the box in panel C′. *hf*, head fold; *rbc*, red blood cells; other abbreviations as before. (A–C, B′) ×350; (A′,C) ×136.

to those that stained with anti-i were visible by phase contrast in the splanchnic mesoderm at stages 14–17, but showed no immunofluorescence with anti-I Step.

Short branch-point structures recognized by anti-I Ma

Without neuraminidase treatment

Negligible fluorescence was observed until about stage 12 when a strong reactivity was seen in the extracellular material beneath the ectoderm (Figs 1E, 7A–C). In the anterior trunk, this was visible over the somites (Fig. 7A). Further caudally it extended beyond the somites, overlying the medial part of the lateral plate mesoderm (Fig. 7B,C).

By stage 17, this subectodermal distribution was still apparent in the trunk over the somites and lateral plate, extending laterally as far as the lateral body folds (Fig. 9D), anteriorly into the head region (Fig. 9B) and caudally into the tail bud (Fig. 9C). At the lateral side of the head, the extracellular material between the ectoderm and the otic vesicle was stained (not shown). At the ventral side of the head region, staining was observed in the apical side of the ectoderm and the apical and basal sides of the forebrain floor (Fig. 9B).

Fluorescence was also seen at the apical and basal sides of the pharyngeal endoderm (Fig. 9A), and at

the basal side of the future floor of the hind gut in the posterior trunk and in the tail bud (Fig. 9C).

After neuraminidase treatment

At stages 1–2, uniform intracellular and focal areas of apical surface immunoreactivity were revealed in the ectoderm of the area pellucida (Fig. 1F). By stage 4 anteroposterior regionalization was becoming apparent, with stronger immunofluorescence anteriorly than posteriorly in the midline. By stage 6, this regionalization appeared to be well established (Fig. 2B,E) with a clear difference between the

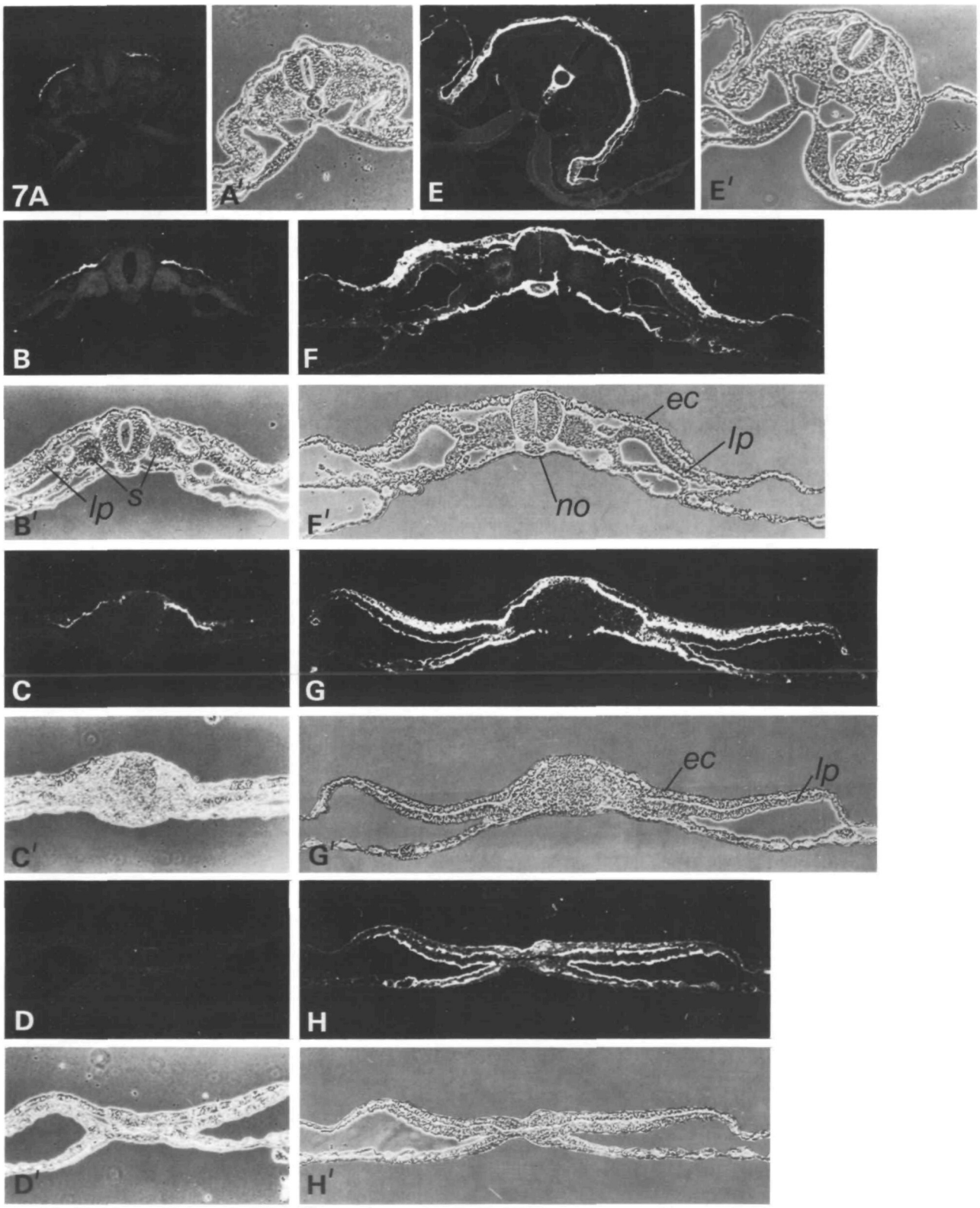

anterior and posterior portions in the midline of the area pellucida. Thus, as the neural plate formed, immunofluorescence became visible at its apical side so that, by the time the neural tube had developed, its apical side was immunostained, especially in the developing brain (Fig. 4B). By stage 14, a localized patch of intra- and pericellular staining was apparent in the floor of the forebrain (Fig. 4B).

The overlying non-neural ectoderm of the embryo, which was barely stained at stage 7, became clearly stained by stage 14 (Fig. 7E–H). The apical side of the ectoderm of the amniotic folds showed immunofluorescence (Fig. 7E) and this was retained in the fully formed amnion (Fig. 4B).

Focal areas of immunoreactivity were revealed at the apical side of the endoderm from about stage 5 onwards (Fig. 2B).

A pronounced immunoreactivity of the apical side of the lateral plate mesoderm was revealed from about stage 7 onwards; this reactivity abruptly ceased in the region of the future lateral body fold.

The intensity of the fluorescence of the subectodermal material was markedly increased after neuraminidase treatment (Fig. 7E–H) and the staining extended further laterally and caudally. Extensive areas of immunoreactivity were revealed by stage 14 in the forebrain region (Fig. 4B), not only in the subectodermal material but also between the mesoderm cells, and on both the basal and apical sides of the lens placodes (Figs 4B, 9E); in the extracellular material between the mesenchyme region of the future pharyngeal arches, between the developing heart and the body wall (Fig. 4B). In addition, there was a very striking immunofluorescence around the notochord from about stage 12 (Fig. 8A) and in the extracellular material at the basal side of the endoderm of the floor of the future gut from about stage 14 (Fig. 7F,G), and to a lesser extent in the intercellular spaces in the ectoderm, and between the mesenchyme cells in the tail bud region (Fig. 7G).

Fig. 7. Fluorescence (A–H) and corresponding phase-contrast (A′–H′) photomicrographs of transverse sections (selected from serial sections) of the midtrunk regions of two stage-14 embryos. They have been stained with anti-I Ma to show the effect of neuraminidase treatment at corresponding levels along the anteroposterior axis. Sections of one embryo (A–D) were untreated, whilst sections of the other embryo (E–H) were neuraminidase treated prior to immunofluorescence staining. Without neuraminidase, staining was restricted to the subectodermal extracellular matrix overlying the somites and the medial part of the lateral plate (A–C). After neuraminidase, this staining extended further laterally and caudally (E–H), and reactivities were revealed around the notochord (E,F), at the apical side of the non-neural ectoderm (E–H) and at the apical side of the lateral plate mesoderm (G,H). *lp*, lateral plate. ×66.

The neural crest cells of the dorsal stream were found to lie beneath the stainable subectodermal material though not surrounded by it, but the neural crest cells of the ventral stream, which were located on either side of the neural tube, were not associated with immunofluorescent extracellular material (Fig. 8).

Short branch-point structures recognized by M18 antibody

The overall pattern of immunofluorescence of untreated and neuraminidase-treated sections with M18 antibody was similar to that observed with anti-I Ma.

Discussion

The salient findings in this study are that carbohydrate antigens of the poly-*N*-acetyllactosamine series are not only prominent in the early chick embryo but they also show a remarkable patterning, with changes at successive developmental stages. In particular, there are distinct anteroposterior, mediolateral and dorsoventral patterns of expression in epithelia and extracellular matrices. The reagents that we have used, antibodies in conjunction with neuraminidase, enable a distinction to be made between (a) long-chain unbranched sequences, reactive with anti-i Den; (b) long-chain branched sequences, reactive with anti-I Step; (c) short-chain branched sequences, reactive with anti-I Ma (Table 2); and (d) their sialylated forms.

Immunofluorescence patterns

Glycosylation patterning in the neural and non-neural ectoderm

The immunofluorescence patterns in the preprimitive-streak-stage embryos observed with anti-i Den (with and without neuraminidase treatment), and with anti-I Step (after neuraminidase treatment) suggest that there is an abundance of the long-chain (poly-*N*-acetyllactosamine) sequences, both linear and branched, of which the branched are the more highly sialylated (shown schematically in Fig. 10A–C). By the time the primitive streak and head process were fully formed, the long-chain branched antigens were no longer detected in the region of the future neural plate (Fig. 10G), though the linear antigens in the sialylated form persisted in this region until about stage 5 or 6 (Fig. 10F); this corresponds to a region where the surface morphology, as assessed by scanning electron microscopy, differs from that of the surrounding ectoderm (Bancroft & Bellairs, 1974). Thereafter, the progressive anteroposterior loss of immunoreactivity suggests either that the long-chain structures are no

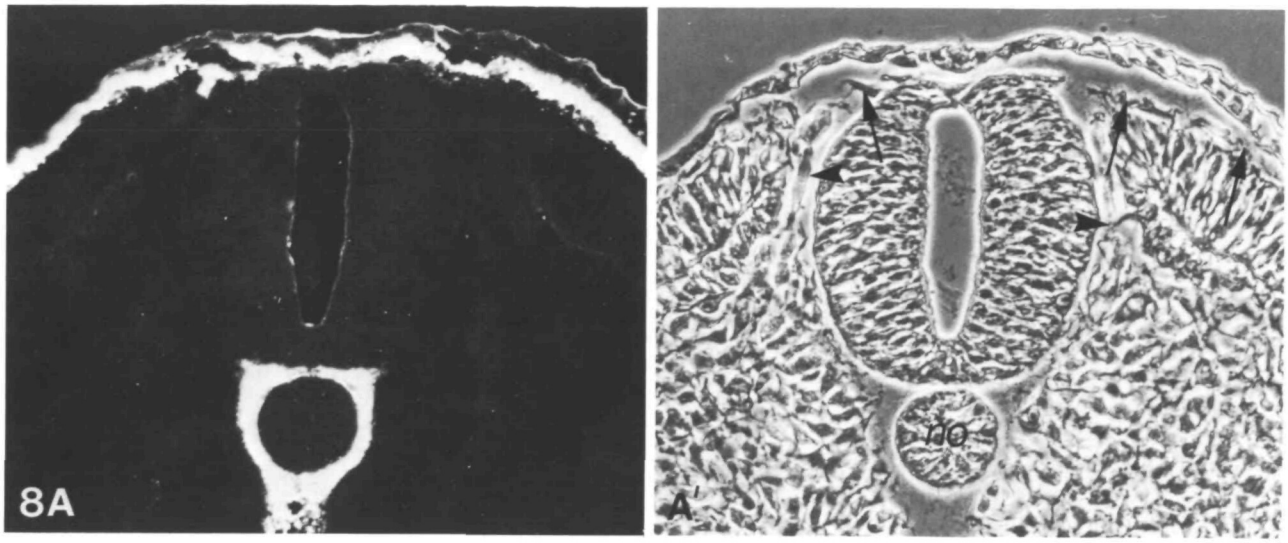

Fig. 8. Enlargements of parts of the fluorescence (A) and corresponding phase-contrast (A′) photomicrographs of the neuraminidase-treated section of a stage-14 embryo shown in Fig. 8E,E′. Neural crest cells of the dorsal stream (arrows) lie beneath the subectodermal material which is stained with anti-I Ma. Neural crest cells of the ventral stream (arrowheads) are not associated with similarly stained material. Also shown is the sharp demarcation of the immunoreactive extracellular material surrounding the notochord. ×318.

longer synthesized or that they are masked by substituents that are not susceptible to digestion with neuraminidase. The changes coincided with the gradual extension of the neural plate along the anteroposterior axis and were still apparent after the closure of the neural tube, so that, by stage 14 and thereafter, the linear structures were detected only at the posterior end of the neural tube.

Coincident with the loss of immunoreactivity of the long-chain structures (i Den and I Step) was the appearance of a reciprocal anteroposterior pattern of ectodermal immunoreactivity with anti-I Ma after neuraminidase treatment (Fig. 10H). This reflected an abundance of the short-chain branched sequences capped with sialic acid (sialosyl-I Ma) in those areas that lack the long-chain structures. Through stages 14–17, there was much stronger reactivity in the developing brain than further posteriorly; this was particularly marked in the floor of the forebrain where, in addition, the nonsialylated I Ma was detected by stage 17.

In the non-neural embryonic ectoderm also there was a progressive increase of the short-chain sialosyl-I Ma and a progressive decrease of the long-chain antigens, especially at the anterior end of the embryo.

A further patterning was evident in the reactivities of the extraembryonic regions of the apical side of the ectoderm; in the earlier stages, long-chain linear and branched antigens were abundantly expressed, whereas the short-chain branched antigens were not detected. At later stages, all three immunoreactivities were apparent in the amniotic folds and subsequently in the amnion. Thus, the antigenic phenotype of the fully formed amnion had characteristics of the ectoderm of the preprimitive-streak stages.

Regional glycosylation patterning in the extracellular spaces

The immunoreactivities of the extracellular spaces showed pronounced regional differences as well as changes during successive stages of development, as summarized in Table 3. For example, at stages 12–14, there were distinct anteroposterior and mediolateral patterns in the carbohydrate structures detected in the subectodermal regions. This is shown schematically in Fig. 11. Anteriorly, in the region of the head, heart and lateral plate mesoderm (somatic layer), there was a predominance of the sialylated short-chain branched structure (sialosyl-I Ma), whereas, posteriorly, the linear long-chain structure (i Den) and the nonsialylated I Ma were detected as well as sialosyl-I Ma. In addition, a mediolateral pattern was evident in that the i Den and nonsialylated I Ma were confined to the region over the proximal part of the lateral plate whereas sialosyl-I Ma extended further laterally. At this stage, the lateral extent of the i-Den and nonsialylated I Ma structures corresponds to the lateral limit of the migration of cells from the primitive streak. This limit marks the future junction between the embryonic and extraembryonic regions (Ooi *et al.* 1986). By stage 17, the pattern of expression of i Den was unchanged but that of nonsialylated I Ma extended anteriorly into the head region and distally over the lateral plate at the posterior end.

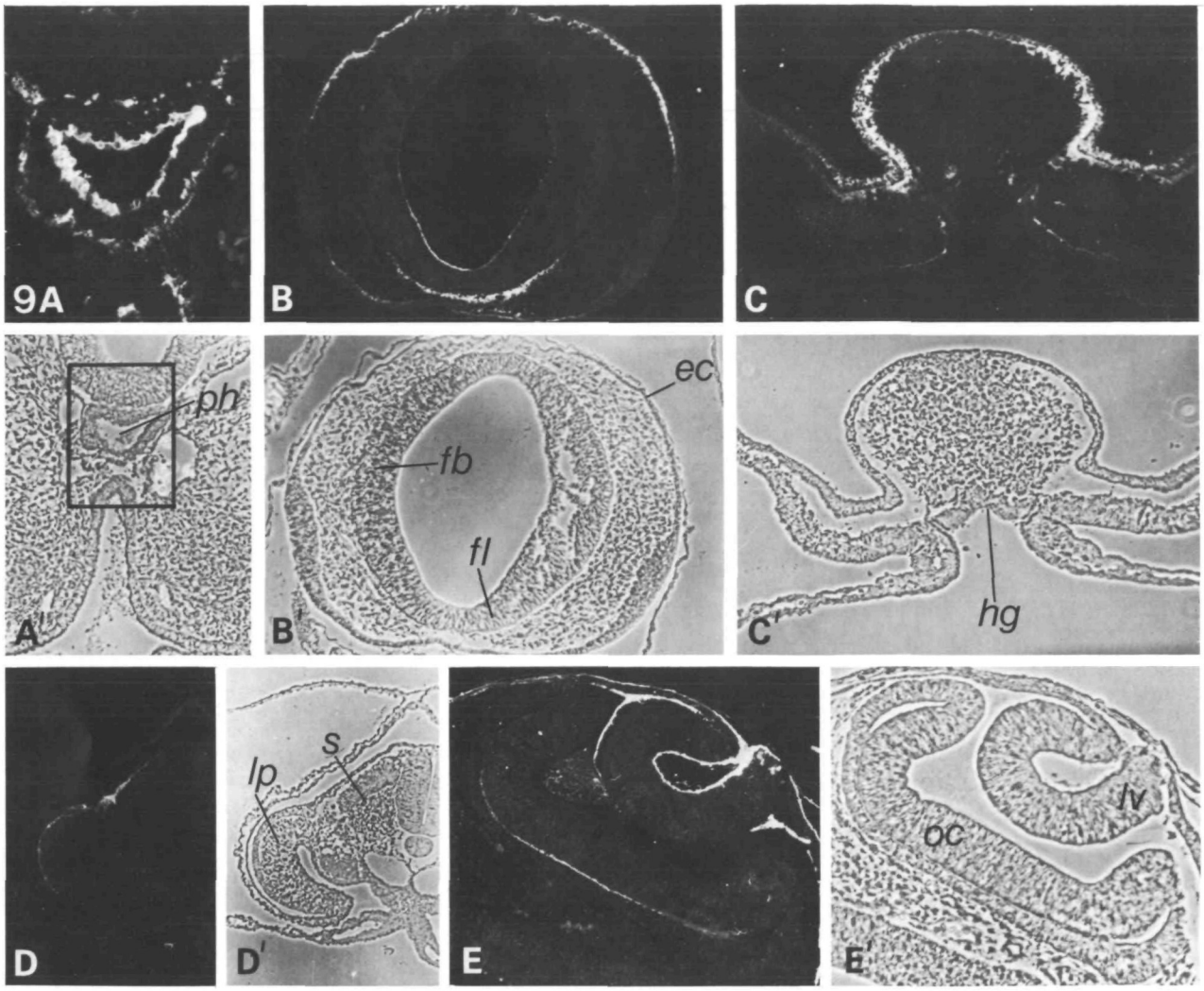

Fig. 9. Fluorescence (A–E) and corresponding phase-contrast (A′–E′) photomicrographs of transverse sections (selected from serial sections) of stage-17 embryos stained with anti-I Ma with (E), and without (A–D), neuraminidase treatment. Even without neuraminidase treatment, extensive staining is visible at the apical and basal sides of the pharynx (A), and at the apical and basal sides of the floor of the forebrain (B), in the extracellular material in the subectodermal region in the head (B), and over the somites and the lateral plate (D). After neuraminidase treatment, the apical and basal aspects of the non-neural ectoderm, including the lens vesicle, show strong immunofluorescence (E). *oc*, optic cup; *lv*, lens vesicle; other abbreviations as before. (A) ×212; (A′) ×88; (B,B′,CC′) ×84; (D,D′) ×65; (E,E′) ×318.

A dorsoventral patterning was evident in the carbohydrate structures detected in the pathways of the trunk neural crest at stage 14: i Den and sialosyl-I Ma structures were found associated exclusively with the extracellular matrix of the dorsal route but not the ventral routes. The relationship of these two immunoreactivities to the neural crest was not always identical, however, i Den being mainly restricted to the levels where neural crest emigration was beginning, whilst nonsialylated I Ma appeared to be associated with crest cells that had already embarked on their migration. Furthermore, the distribution of I Ma in the head regions at stage 17 (when emigration has already taken place) corresponded with that of the cranial neural crest during the course of its migration (Noden, 1984).

Around the notochord, a striking compartmentation of the sialosyl-I Ma structure in the extracellular space was revealed, the limits of which correspond to the future centra of the vertebrae.

Regional differences were observed also in the glycosylation of the extracellular space at the basal side of the endoderm: at stage 14, i Den was detected exclusively at the posterior end, whereas sialosyl-I Ma was present throughout. By stage 17, I Ma could be detected in the nonsialylated form beneath the extreme anterior and posterior ends of the gut endoderm.

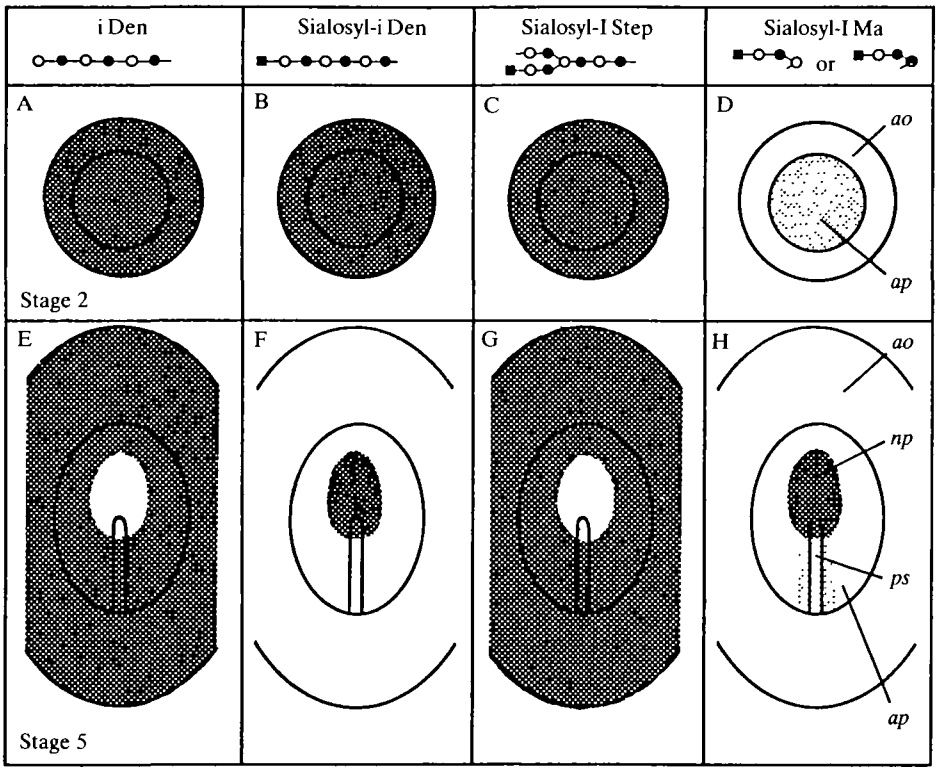

Fig. 10. Schematic presentation of the apical side of the ectoderm of the chick embryo at stage 2 (panels A–D) and stage 5 (E–H) to show the changes in distribution of the linear (i Den and sialosyl-i Den) and branched (sialosyl-I Step and sialosyl-I Ma) structures. The presence of the sialosyl structures in panels B–D and F–H was deduced from enhancement or the revealing of new immunoreactivities after neuraminidase treatment of the sections. Shaded areas indicate strong or moderate (□) and weak (□) immunoreactivities. Abbreviations: *ap*, area pellucida; other abbreviations are as before. Symbols: ■, sialic acid; ○, galactose; ●, *N*-acetylglucosamine; ◉, *N*-acetylgalactosamine.

Table 3. *Carbohydrate structures deduced to be present in extracellular spaces of chick embryos up to stage 17*

Region	i-Den	I Ma	Sialosyl-I Ma
Subectodermal			
head region		17*	14
heart region			+
over somites	$+^{P}$	12	+
over lat. pl. (proximal)	$+^{P}$	12^{P}	+
over lat. pl. (distal)		17^{P}	+
over neural crest (dorsal)	14		+
tail bud	$+^{l}$	17	+
Between mesenchyme cells (head and pharynx)			+
Between sclerotome cells	17		
Around notochord	(+)		(12)
Between tail bud cells	+		14
Subendodermal	14^{P}	$17^{*,P}$	14

*Symbols: + = antigen detected during stages examined; (+) antigen patchily expressed; numbers (e.g. 12, 14) indicate earliest embryonic stages at which immunoreactivities were detected. Abbreviations for immunoreactivities at restricted regions: *, anterior; ^{P}, posterior; ^{l}, lateral folds.

There was a notable lack of expression of the long-branched antigen (I Step) in the extracellular matrices.

Other glycosylation patterns

At the apical side of the endoderm, the sialosyl-I Ma structure was detected throughout the embryo from

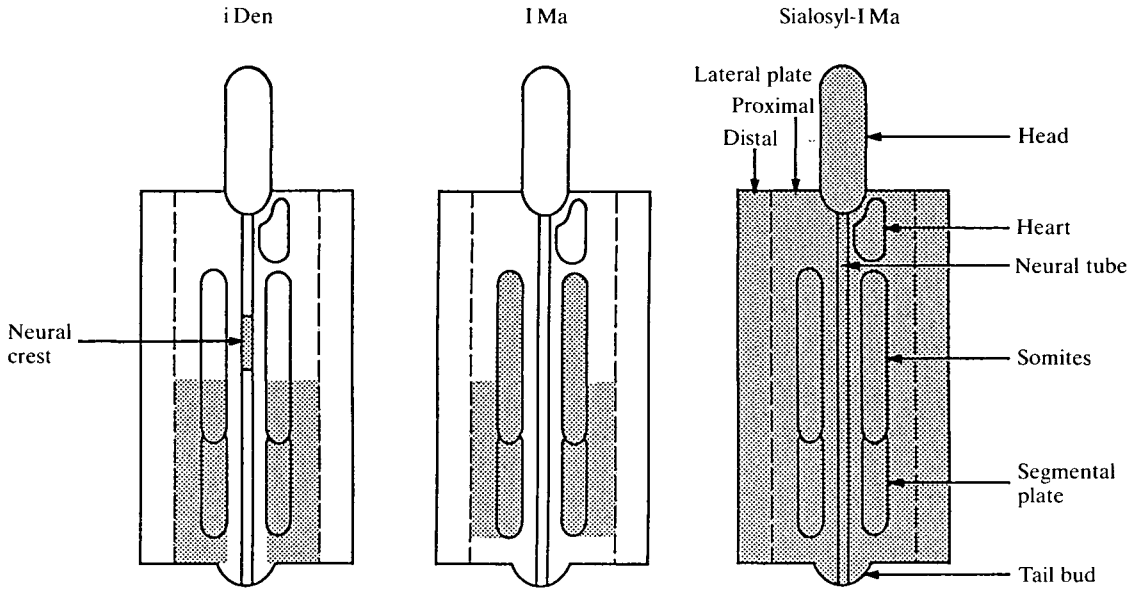

Fig. 11. Schematic presentation of the subectodermal extracellular space of the chick embryo at stage 12–14 showing the differing anteroposterior and mediolateral patterns of distribution of the linear (i Den), and the short-branched (I Ma and sialosyl-I Ma) structures. The presence of the sialosyl-I Ma structure was deduced from enhancement or the revealing of new immunoreactivities after neuraminidase treatment of the sections.

stage 5 onwards. However, an anteroposterior pattern was apparent with nonsialylated-I Ma which was predominantly detected at the anterior end, and the linear i Den sequence at the posterior end. At the apical side of the lateral plate, sialosyl-I Ma only was detected. The primordial germ cells were associated with the linear (i Den) and branched (sialosyl-I Step) long-chain structures but not the short-chain branched structure.

Biological relevance

The abundance of carbohydrate structures of the poly-*N*-acetyllactosamine series shown here in the chick embryo, and in the mouse and human embryos (Muramatsu *et al.* 1980; Kapadia *et al.* 1981; Fukushi *et al.* 1984; Pennington *et al.* 1985), and their striking changes in distribution during development, suggest a fundamental role for these structures during early embryogenesis. A great diversity of oligosaccharide structures can arise both from changes in chain length and branching patterns of the backbone regions and from their peripheral substitutions (Feizi, 1985) and one of the greatest challenges for the future is to unravel their biological information content. It has previously been suggested that each substitution to the backbone structures may confer a specific function; by interacting with complementary structures on adjacent cells or matrices they may play a critical role in guiding cell migration or influencing cell orientation (Feizi, 1980; Kapadia *et al.* 1981; Feizi & Childs, 1985), or they may interact with endogenous growth regulatory molecules (Feizi, 1982; Feizi *et al.* 1982; Feizi & Childs, 1985, 1987). In the mouse, the demonstration that the stage-specific embryonic antigen, SSEA-1 (which first appears at the compaction stage) is formed by the addition of fucose in α1–3 linkage to *N*-acetylglucosamine residues of poly-*N*-acetyllactosamine sequences, led to the proposal that these structures may be involved in the compaction of the blastomeres (Gooi *et al.* 1981). Experiments designed to test this hypothesis have provided evidence for the involvement of oligosaccharides of the poly-*N*-acetyllactosamine series in the compaction process (Rastan *et al.* 1985), although the role of the SSEA-1 structure *per se* requires further investigation (Bird & Kimber, 1984; Fenderson *et al.* 1984; Feizi, 1985). In sensory neurones of the neonatal and adult rat, there is a coincidence of immunohistochemical staining by antibodies to β-galactoside binding endogenous lectins and to *N*-acetyllactosamine (Regan *et al.* 1986) and poly-*N*-acetyllactosamine sequences (J. Dodd, T. M. Jessel & T. Feizi, unpublished observations). This is suggestive of a role for specific sugar–protein interactions as recognition signals in neural development and function.

The striking temporal and regional patterning of carbohydrate antigenicity observed in the present series suggests that carbohydrate structures of the poly-*N*-acetyllactosamine series may have important roles during the morphogenetic events in the chick embryo also. Specific questions can now be asked about the information content of individual oligosaccharide structures, particularly in the following contexts.

(1) In the developing brain, the abrupt disappearance of the long-chain antigens (i Den and sialosyl-I Step) coincidental with the appearance of the short-chain branched antigen, sialosyl-I Ma, suggests that short-chain *O*-glycosidically linked oligosaccharides (analogues of structure 5, Table 2) may be selectively accumulating during neuroectodermal differentiation. The pericellular accentuation of sialosyl-I Ma at restricted sites, such as the floor of the forebrain at stages 14–17, raises the possibility that it may be associated with cell adhesion molecules at restricted sites.

(2) Subectodermal extracellular spaces containing i Den and/or I Ma may correspond to regions favourable for the migration of lateral plate embryonic mesoderm.

(3) In the microenvironment of the neural crest, where extracellular matrix components such as glycosaminoglycans may play a major part in cell migration (Weston *et al.* 1984; Newgreen & Erickson, 1986; Sanders, 1986), i Den and sialosyl-I Ma may provide cues to particular migration routes.

(4) The striking perinotochordal distribution of sialosyl-I Ma suggests that this structure may be an additional member of the proposed family of short-range factors, such as glycosaminoglycans (Vasan, 1981; Oettinger *et al.* 1985) which by chemoattraction or other mechanisms may promote the migration and differentiation of sclerotome cells at chondrogenic sites.

(5) The abundance of long-chain poly-*N*-acetyllactosamine structures (i Den and sialosyl-I Step) in the primordial germ cells which enables these cells to be readily identified, will greatly facilitate detailed studies of their developmental programming during migration.

Future studies will be directed at identifying the cellular origins and macromolecular carriers of these carbohydrate structures. The candidate carrier molecules include fibronectins and laminins, which in certain human embryonic tissues (Zhu & Laine, 1985) and rat tumour tissues (Arumugham *et al.* 1986), respectively, have been shown to have oligosaccharides of the poly-*N*-acetyllactosamine series. However, any proposals for the functions of oligosaccharides of this series must take into account that they are not confined to extracellular matrices and cell contact sites, but they are also prominent at apical aspects of epithelia as shown in the present and earlier studies, and they occur on integral membrane glycoproteins. Some well-established glycoproteins that carry these antigens on cell membranes include brush border enzymes, a glycosyltransferase, anion and sugar transport proteins and the glycoprotein receptor for epidermal growth factor (reviewed by Feizi & Childs, 1987). Thus future studies will, in addition, focus on identifying the recognition proteins (e.g. endogenous lectins) with which the individual oligosaccharides react in these various locations. Prospects for identifying such recognition systems are now improved, for it should be possible in the near future to use oligosaccharide probes derived from the embryonic tissues, in the form of neoglycolipids or neoglycoproteins (Tang *et al.* 1985; Tang & Feizi, 1987) and to design methods for evaluating their reactions with various components in the organizing tissues or with individual purified proteins derived from them. Knowledge of the *in situ* distribution of specific oligosaccharide sequences is therefore an important guide to the design of experiments to decode their information content.

S.J.T. was supported by the Cancer Research Campaign. This work was supported in part by grants from Action Research for the Crippled Child and the British Heart Foundation to R.B. The authors are grateful to Maureen Moriarty and Margaret Runnicles for typing the manuscript.

References

Arumugham, R. G., Hsieh, T. C.-Y., Tanzer, M. L. & Laine, A. (1986). Structures of the asparagine-linked sugar chains of laminin. *Biochim. biophys. Acta* **883**, 112–126.

Bancroft, M. & Bellairs, R. (1974). The onset of differentiation in the epiblast of the chick blastoderm (SEM and TEM). *Cell Tiss. Res.* **155**, 399–418.

Bird, J. M. & Kimber, S. J. (1984). Oligosaccharides containing fucose linked $\alpha(1-3)$ and $\alpha(1-4)$ to *N*-acetylglucosamine cause decompaction of mouse morulae. *Devl Biol.* **104**, 449–460.

Childs, R. A., Kapadia, A. & Feizi, T. (1979). Blood group I and i antigens as common surface antigens on a variety of human and animal cell lines. In *Glycoconjugates* (ed. R. Schauer, P. Boer, E. Buddecke, M. F. Kramer, J. F. G. Vliegenthart, & H. Wiegandt), pp. 518–519. Stuttgart: Georg Thieme Publishers.

Childs, R. A., Kapadia, A. & Feizi, T. (1980). Expression of blood group I and i active carbohydrate sequences on cultured human and animal cell lines assessed by radioimmunoassays with monoclonal cold agglutinins. *Eur. J. Immun.* **10**, 379–384.

Drury, R. A. B. & Wallington, E. A. (1967). *Carlton's Histological Technique.* Oxford University Press.

Feizi, T. (1980). Structural and biological aspects of blood group I and i antigens on glycolipids and glycoproteins. *Blood Trans. Immunohaematol.* **23**, 563–577.

Feizi, T. (1981*a*). The blood group Ii system: a carbohydrate antigen system defined by naturally monoclonal or oligoclonal autoantibodies of man. *Immunol. Commun.* **10**, 127–156.

FEIZI, T. (1981*b*). Carbohydrate differentiation antigens. *Trends Biochem. Sci.* **6**, 333–335.

FEIZI, T. (1982). The antigens Ii, SSEA-1 and ABH are an interrelated system of carbohydrate differentiation antigens expressed on glycosphingolipids and glycoproteins. *Adv. exp. Med. Biol.* **152**, 167–177.

FEIZI, T. (1985). Demonstration by monoclonal antibodies that carbohydrate structures of glycoproteins and glycolipids are onco-developmental antigens. *Nature, Lond.* **314**, 53–57.

FEIZI, T. & CHILDS, R. A. (1985). Carbohydrate structures of glycoproteins and glycolipids as differentiation antigens, tumour-associated antigens and components of receptor systems. *Trends in Biochem. Sci.* **10**, 24–29.

FEIZI, T. & CHILDS, R. A. (1987). Carbohydrates as antigenic determinants of glycoproteins. *Biochem. J.* **245**, 1–11.

FEIZI, T., CHILDS, R. A., WATANABE, K. & HAKOMORI, S. (1979). Three types of blood group I specificity among monoclonal anti-I autoantibodies revealed by analogues of a branched erythrocyte glycolipid. *J. exp. Med.* **149**, 975–980.

FEIZI, T., KABAT, E. A., VICARI, G., ANDERSON, B. & MARSH, W. L. (1971). Immunochemical studies on blood groups XLIX. The I antigen complex: specificity differences among anti-I sera revealed by quantitative precipitin studies; partial structure of the I determinant specific for one anti-I serum. *J. Immun.* **106**, 1578–1592.

FEIZI, T., KAPADIA, A., GOOI, H. C. & EVANS, M. J. (1982). Human monoclonal autoantibodies detect changes in expression and polarization of the Ii antigens during cell differentiation in early mouse embryos and teratocarcinomas. In *Teratocarcinoma and Embryonic Cell Interactions* (ed. T. Muramatsu, G. Gachelin, A. Moscona, Y. Ikawa), pp. 201–215. Tokyo: Japan Scientific Societies Press & Academic Press.

FENDERSON, B. A., ZEHAVI, U. & HAKOMORI, S. (1984). A multivalent lacto-N-fucopentaose III–lysyllysine conjugate decompacts preimplantation-stage mouse embryos while the free oligosaccharide is ineffective. *J. exp. Med.* **160**, 1591–1596.

FUKUSHI, Y., HAKOMORI, S. & SHEPARD, T. (1984). Localization and alteration of mono-, di-, and trifucosyl α1-3 Type 2 chain structures during human embryogenesis and in human cancer. *J. exp. Med.* **159**, 506–520.

GOOI, H. C., FEIZI, T., KAPADIA, A., KNOWLES, B. B., SOLTER, D. & EVANS, M. J. (1981). Stage specific embryonic antigen SSEA-1 involves α1-3 fucosylated Type 2 blood group chains. *Nature, Lond.* **292**, 156–158.

GOOI, H. C., UEMURA, K., EDWARDS, P. A. W., FOSTER, C. S., PICKERING, N. & FEIZI, T. (1983). Two mouse hybridoma antibodies against human milk fat globules recognise the I(Ma) antigenic determinant: Galβ1-4GlcNAcβ1-6–. *Carbohydr. Res.* **120**, 293–302.

GOOI, H. C., VEYRIÈRES, A., ALAIS, J., SCUDDER, P., HOUNSELL, E. F. & FEIZI, T. (1984). Further studies of the specificities of monoclonal anti-i and anti-I antibodies using chemically synthesized, linear oligosaccharides of the poly-*N*-acetyllactosamine series. *Molec. Immunol.* **21**, 1099–1104.

HAKOMORI, S. (1981). Blood group ABH and Ii antigens of human erythrocytes: chemistry, polymorphism and their developmental change. *Semin. Hematol.* **18**, 39–62.

HAMBURGER, V. & HAMILTON, H. L. (1951). A series of normal stages in the development of the chick embryo. *J. Morph.* **88**, 49–92.

JOHNSON, G. D., DAVIDSON, R. S., MCNAMEE, K. C., RUSSELL, G., GOODWIN, D., HOLBOROW, E. J. (1982). Fading of immunofluorescence during microscopy: a study of the phenomenon and its remedy. *J. Immunol. Methods* **55**, 231–242.

KAPADIA, A., FEIZI, T. & EVANS, M. J. (1981). Changes in the expression and polarization of blood group I and i antigens in post-implantation embryos and teratocarcinomas of mouse associated with cell differentiation. *Expl Cell Res.* **131**, 185–195.

MURAMATSU, T., CONDAMINE, H., GACHELIN, G. & JACOB, F. (1980). Changes in fucosyl-glycopeptides during early post-implantation embryogenesis in the mouse. *J. Embryol. exp. Morph.* **57**, 25–36.

NEWGREEN, D. F. & ERICKSON, C. A. (1986). The migration of neural crest cells. *Int. Rev. Cytol.* **103**, 89–145.

NIEMANN, H., WATANABE, K., HAKOMORI, S., CHILDS, R. A. & FEIZI, T. (1978). Blood group i and I activities of "Lacto-N-*nor*hexaosyl ceramide" and its analogues: the structural requirements for i-specificities. *Biochem. biophys. Res. Commun.* **81**, 1286–1293.

NODEN, D. M. (1984). Craniofacial development: new views on old problems. *Anat. Rec.* **208**, 1–13.

OETTINGER, H. F., THAL, G., SASSE, J., HOLTZER, H. & PACIFICI, M. (1985). Immunological analysis of chick notochord and cartilage matrix development with antisera to cartilage matrix macromolecules. *Devl Biol.* **109**, 63–71.

OOI, V. E. C., SANDERS, E. J. & BELLAIRS, R. (1986). The contribution of the primitive streak to the somites in the avian embryo. *J. Embryol. exp. Morph.* **92**, 193–206.

PANNETT, C. A. & COMPTON, A. (1924). The cultivation of tissues in saline embryonic juice. *Lancet* **1**, 381–384.

PENNINGTON, J. E., RASTAN, S., ROELCKE, D. & FEIZI, T. (1985). Saccharide structures of the mouse embryo during the first eight days of development. *J. Embryol. exp. Morph.* **90**, 335–361.

RASTAN, S., THORPE, S. J., SCUDDER, P., BROWN, S., GOOI, H. C. & FEIZI, T. (1985). Cell interactions in preimplantation embryos: evidence for involvement of saccharides of the poly-*N*-acetyllactosamine series. *J. Embryol. exp. Morph.* **87**, 115–128.

REGAN, L. J., DODD, J., BARONDES, S. H. & JESSELL, T. M. (1986). Selective expression of endogenous lactose binding lectins and lactoseries glycoconjugates in subsets of rat sensory neurones. *Proc. natn. Acad. Sci. U.S.A.* **83**, 2248–2252.

SANDERS, E. J. (1986). Cytochemistry of the cell surface and extracellular matrix during early embryonic development. *Prog. Histochem. Cytochem.* **16**, 1–57.

TANG, P. W. & FEIZI, T. (1987). Neoglycolipid micro-immunoassays applied to the oligosaccharides of human milk galactosyltransferase detect blood group related antigens on both O- and N-linked chains. *Carbohydr. Res.* **161**, 133–143.

TANG, P. W., GOOI, H. C., HARDY, M., LEE, Y. C. & FEIZI, T. (1985). Novel approach to the study of the antigenicities and receptor functions of carbohydrate chains of glycoproteins. *Biochem. biophys. Res. Commun.* **132**, 474–480.

THORPE, S. J. & FEIZI, T. (1983). Blood group antigens in the normal and neoplastic bladder epithelium. *J. clin. Path.* **36**, 873–883.

UEMURA, K., CHILDS, R. A., HANFLAND, P. & FEIZI, T. (1983). A multiplicity of erythrocyte glycolipids of the neolacto series revealed by immuno-thin layer chromatography with monoclonal anti-I and anti-i antibodies. *Biosci. Reps.* **3**, 577–588.

VASAN, N. (1981). Analysis of perinotochordal materials. 1. Studies on proteoglycan synthesis. *J. exp. Zool.* **215**, 229–233.

WESTON, J. A., CIMENT, G. & GIRDLESTONE, J. (1984). The role of extracellular matrix in neural crest development: a re-evaluation. In *The Role of Extra-Cellular Matrix in Development* (ed. R. L. Trelstad), pp. 433–460. New York: Alan Liss.

ZHU, B. C. R. & LAINE, R. A. (1985). Polylactosamine glycosylation on human fetal placental fibronectin weakens the binding affinity of fibronectin to gelatin. *J. biol. Chem.* **260**, 4041–4045.

(*Accepted 10 October 1987*)